Telomere associations in interphase nuclei: possible role in maintenance of interphase chromosome topology

Robert G. Nagele[1,*], Antonio Q. Velasco[2], William J. Anderson[2], Donald J. McMahon[2], Zabrina Thomson[2], Jessica Fazekas[1], Kelly Wind[1] and Hsin-yi Lee[2]

[1]Department of Molecular Biology, University of Medicine and Dentistry of New Jersey – School of Osteopathic Medicine, Stratford, New Jersey 08084, USA
[2]Department of Biology, Rutgers University, Camden, New Jersey, 08102, USA
*Author for correspondence (e-mail: nagelero@umdnj.edu)

Accepted 27 October 2000
Journal of Cell Science 114, 377-388 © The Company of Biologists Ltd

SUMMARY

The relative sizes of individual telomeres in cultured human cells under conditions of cell cycling, replicative quiescence, cell transformation and immortalization were determined using quantitative fluorescence in situ hybridization (Q-FISH) with a telomere-specific peptide nucleic acid (PNA) probe. Results obtained from analysis of telomere length profiles (TLPs), which display the distribution of relative telomere lengths for individual cells, confirmed telomere length heterogeneity at the single cell level and proportional shortening of telomere length during replicative aging of virus-transformed cells. TLPs also revealed that some telomeric ends of chromosomes are so closely juxtaposed within interphase nuclei that their fluorescent signals appear as a single spot. These telomeric associations (TAs) were far more prevalent in interphase nuclei of noncycling normal and virus-transformed cells than in their cycling counterparts. The number of interphase TAs per nucleus observed in late-passage E6/E7-transformed cells did not increase during progression to crisis, suggesting that telomere shortening does not increase the frequency of interphase TAs. Furthermore, interphase TAs were rarely observed in rapidly cycling, telomerase-positive, immortalized cells that exhibit somewhat shortened, but stabilized, telomere length through the activity of telomerase. Our overall results suggest that the number of interphase TAs is dependent more on whether or not cells are cycling than on telomere length, with TAs being most prominent in the nuclei of replicatively quiescent cells in which nonrandom (even preferred) chromosome spatial arrangements have been observed. We propose that interphase TAs may play a role in the generation and/or maintenance of nuclear architecture and chromosome positional stability in interphase nuclei, especially in cells with a prolonged G_1/G_0 phase and possibly in terminally differentiated cells.

Key words: Telomere, Telomere shortening, Telomere association, Chromosome end fusion

INTRODUCTION

Strong evidence is emerging that chromosomes are not randomly arranged throughout the cell cycle. For example, chromosomes arrange themselves into a wheel-like array, referred to as a rosette, in mitotic cells from a variety of species, and maintain this configuration from prometaphase through completion of mitosis (Costello, 1970; DuPraw, 1970; Heslop-Harrison and Bennett, 1984; Chaly and Brown, 1988; Nagele et al., 1995; Klein et al., 1998; Nagele et al., 1998; Nagele et al., 1999). Chromosome homologs show a remarkable tendency to be positioned on opposite sides of the circular rosette (Nagele et al., 1995; Nagele et al., 1998; Koss et al., 1998; Sun and Yokota, 1999). In interphase nuclei, chromosomes occupy discrete, non-overlapping territories that are nonrandomly distributed in many animal and plant cells (Comings, 1968; Comings, 1980; Heslop-Harrison and Bennett, 1984; Manuelidis, 1984; Manuelidis, 1990; Haaf and Schmid, 1991; Mosgoller et al., 1991; Spector, 1993, Leitch et al., 1994; Leitch, 2000). For example, we have recently shown that chromosomes 7, 8, 16, X and Y occupy preferred positions within the interphase nuclei of quiescent (noncycling) cultured human fibroblasts and that their relative locations are related directly to their positions within chromosome rosettes (Nagele et al., 1999). Recent studies have also shown that the specific intranuclear positions of some chromosomes may be established early in the cell cycle and that the organization of chromosomes in quiescent and senescent cells is fundamentally different from that seen in proliferating cells (Croft et al., 1999; Bridger et al., 2000). Nonrandom distributions of interphase chromosomes are not unique to cultured cells. Manuelidis and Borden (1988) have shown that some chromosome domains exhibit similar intranuclear distribution patterns in human and mouse central nervous system cells. Consistent chromosome positions are maintained throughout the cell cycle in normal human bronchial epithelial cells in vivo (Koss et al., 1998). A symmetrical chromosome arrangement has been demonstrated in both interphase and mitotic leukocytes (Chaudhuri and Reith, 1997). Also, separation of parental haploid chromosome sets has been

described in several systems (Leitch et al., 1991; Heslop-Harrison and Bennett, 1984; Bennett and Bennett, 1992; Schwarzacher et al., 1992; Callimassia et al., 1994; Nagele et al., 1995; Nagele et al., 1998; Mayer et al., 2000).

Despite evidence for an organized chromosome topology in interphase nuclei, factors that mediate and regulate this phenomenon remain elusive. Some studies have suggested that components of the nuclear matrix anchor chromosomes or chromosomal subunits to their preferred intranuclear positions (Mirkovitch et al., 1984; Berezney, 1991; Craig et al., 1997; Nickerson et al., 1997; Weipoltshammer et al., 1999). Telomeres and telomere-specific binding proteins may associate with the nuclear matrix and participate in anchoring chromosomes (de Lange, 1992; Luderus et al., 1996; Weipoltshammer et al., 2000). Telomeres consist of a highly conserved, repetitive hexanucleotide sequence (TTAGGG in mammals), which associates with several specific proteins that cap the ends of chromosomes (Hastie and Allshire, 1989; Meyne et al., 1989; de Lange et al., 1990; Blackburn, 1991; Zakian, 1995; van Steensel et al., 1998). Telomere integrity is essential for chromosome numerical and positional stability, and telomere shortening appears to facilitate the evolution of cancer cells by promoting chromosome end-to-end fusions and the development of aneuploidy (McClintock, 1941; Zakian, 1989; Hastie and Allshire, 1989; Blackburn, 1991; Harley et al., 1990; Sandell and Zakian, 1993; de Lange, 1995; Blasco et al., 1997; Slijepcevic et al., 1997; Van Steensel et al., 1998). The intersection of dicentric chromosomes at their telomeric ends (telomere associations; TAs) are characterized by the markedly reduced number of telomere repeats (Wan et al., 1999; Hande et al., 1999; Sprung et al., 1999a).

In view of the propensity for the ends of chromosomes to fuse with one another in mitotic cells, a question arises as to whether or not TAs also occur in interphase nuclei. To address this question, we used quantitative fluorescence in situ hybridization (Q-FISH) to directly visualize individual telomeres and detect changes in their relative length at the single telomere and single cell levels (Lansdorp et al., 1996; Zijlmans et al., 1997; Poon et al., 1999; Martens et al., 2000). Telomere length profiles (TLPs), which display the distribution of telomere lengths in single cells, were compared under conditions of replicative quiescence, telomere shortening following bypass of senescence to crisis, and immortalization. Our results show that TAs are common in interphase nuclei and are far more prevalent in quiescent (noncycling) cells than in their cycling counterparts. Since the incidence of TAs in mitotic cells is known to increase dramatically during telomere shortening (Zakian, 1989; Hastie and Allshire, 1989; Blackburn, 1991; Harley et al., 1990; Sandell and Zakian, 1993; de Lange, 1995; Blasco et al., 1997), we expected that the number of TAs observed in interphase nuclei would similarly increase in cells possessing shortened telomeres. However, analysis of TLPs in virus-transformed cells during progression to crisis did not support a correlation between telomere shortening and the number of interphase TAs observed per cell nucleus. Thus, the number of TAs in interphase nuclei is more dependent on the cycling status of the cell, rather than on individual telomere length. In support of this possibility, TAs were only rarely observed in the interphase nuclei of rapidly cycling, telomerase-positive immortalized cells with shortened, but stable, telomere lengths. Since TAs are most prominent in quiescent cells that exhibit preferred positioning of some of their chromosomes (Nagele et al., 1999), they may be involved in the maintenance of chromosome positional stability in interphase nuclei, especially in cells that are proliferating slowly (i.e. a prolonged G_1 phase), replicatively quiescent or terminally differentiated.

MATERIALS AND METHODS

Cell culture

The following cell lines were used in this study: normal human diploid fibroblasts; AG07715, IMR90 human fetal lung fibroblast (PDL 7 and 25) and IMR91 (PDL 13 and 30) (Coriell National Cell Repository); preimmortal E6/E7 virus-transformed cells (kindly provided by Dr Shawn Holt) and HeLa S3 cells. Cells were grown in flasks or on chamber slides (Labtek) in Dulbecco's Modified Eagle Medium (DMEM) (Gibco, BRL) containing 10% fetal calf serum (Gibco, BRL) and 2% penicillin/streptomycin at 37°C in a 5% CO_2 atmosphere. Some cultures (IMR90 and IMR91) were grown to a state of 'high-density confluence' and maintained in this condition for 2-4 days without medium change. This procedure 'locked' these cells in the G_1/G_0 phase of the cell cycle (replicative quiescence) and effectively minimized individual cell and nuclear shape variations that would otherwise have arisen as a result of complex behaviors such as cell migration, cell spreading and mitosis. Confirmation of cell cycle arrest was obtained by the lack of mitotic figures and cell cycle analysis profiles through DNA quantitation using the Cell Analysis System 2000 (CAS 2000, Beckman) as described previously (Nagele et al., 1999). The CAS 2000 system employs a stoichiometric Feulgen staining reaction and microscopic densitometry to determine the total DNA content.

Fluorescence in situ hybridization (FISH) and digital imaging

Cells grown on chamber slides were fixed in 4% paraformaldehyde in phosphate-buffered saline (PBS; 137 mM NaCl, 3 mM KCl, 16 mM Na_2HPO_4, 2 mM $KHPO_4$, pH 7.3) for 20 minutes at room temperature and dehydrated in a graded series of ethanols. Fixed specimens were washed briefly in PBS, followed by three rinses in 2× SSC (1× SSC; 150 mM NaCl, 30 mM sodium citrate) for 10 minutes at room temperature. Cells were treated with 20 μl of Cy3-labeled, telomere-specific $(C_3TA_2)_3$ peptide nucleic acid (PNA) probe (4 ng/μl) (PBIO/Biosearch Product, Bedford, MA, USA) containing 70% formamide/2× SSC, covered with a 22 mm glass coverslip and sealed with rubber cement. This small PNA probe was used because it readily penetrates into the cell and nucleus, exhibits a high degree of stability and yields a fluorescence signal intensity that is directly proportional to the amount of hybridized target (Egholm et al., 1993; Lansdorp et al., 1996; Slijepcevic et al., 1997; Zjilmans et al., 1997). Both probe and cellular DNA were codenatured at 95°C for 10 minutes on a heat block and hybridized overnight in a moist chamber at 37°C. After hybridization, specimens were washed at stringencies recommended by the manufacturer. No detection or amplification steps were necessary because the probe was internally labeled. After three washes in SSC-Tween buffer, cells were mounted in Vectashield mounting solution (Vector Laboratories) containing DAPI as a DNA counterstain. Specimens were examined with a Nikon FXA microscope equipped with epifluorescence optics using a ×60, 1.40 numerical aperture, objective lens and a Princeton Instruments CCD camera. Digital images of telomeres were collected separately under constant exposure conditions. Telomeres were identified through segmentation of the DAPI and Cy3 images. The DAPI image was used to define the morphological boundary of each nucleus. Fading of images was negligible because of the short exposure time and the presence of anti-fading agent in the mounting medium. Variations in

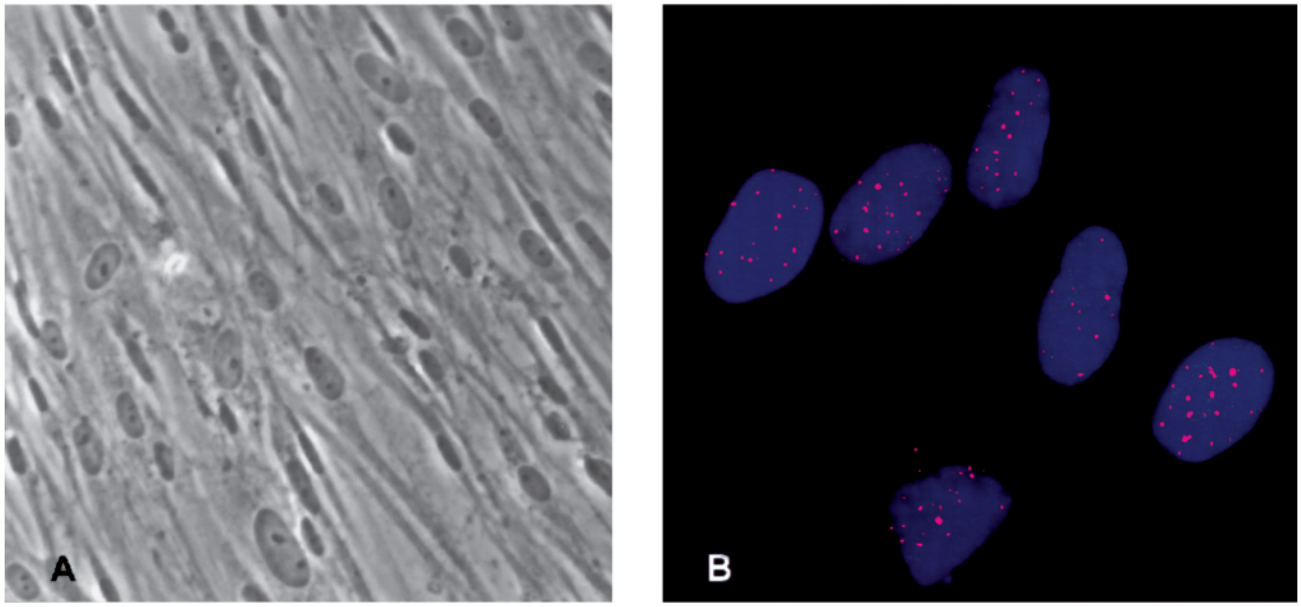

Fig. 1. (A) Phase-contrast image of quiescent diploid human fibroblasts under conditions of high density confluence. (B) Distribution of telomeres (red) in the nuclei (blue) of quiescent fibroblasts.

the signal intensity of telomeres due to daily fluctuations in ultraviolet bulb brightness were corrected by recording the intensity of fluorescent orange bead standards (size 0.2 μm; Molecular Probes) at the beginning of each operator session (Lansdorp et al., 1996). We measured the integrated optical density (IOD) (which factors in both the size and luminosity of the telomere signal) of each telomere using the Image Pro Plus image analysis program (Media Cybernetics). For all measurements, the boundary of each telomere was defined manually, rather than automatically. Our preliminary studies have shown that manual selection of the telomere boundary, although considerably more time-consuming, increases the precision and reproducibility of telomere length measurements over those obtained when telomere boundaries are determined automatically. Replicate measurements carried out by the same and/or different operators verified the accuracy and reproducibility of our measurement strategy. For analysis of the three-dimensional (3D) distribution of telomeres in nuclei, individual optical sections were digitized and 3D-reconstructed using Metamorph (Universal Imaging). Resulting images were examined and presented as stereopairs. To illustrate the distribution of telomeres within the plane of each optical section, individual telomeres and the boundary of the nucleus occurring at each optical section were traced using a digitizing tablet (GTCO Digipad 5) and optical sections were 3D-reconstructed using PC3D (Jandel Scientific) (Nagele et al., 1992). Images were retrieved from hard disks and printed using a Sony dye-sublimation printer. Some fluorescent images were recorded on film, using either Kodak T-Max 400 black-and-white film or Fujichrome 400 color film.

RESULTS

Telomere length profiles of individual, quiescent (noncycling) human fibroblasts

To investigate the relative lengths of single telomeres and generate telomere length profiles (TLPs) for individual normal human fibroblasts, we used the Q-FISH method developed by Lansdorp and coworkers (Lansdorp et al., 1996; Zijlmans et al., 1996; Poon et al., 1999) with minor modifications. To minimize the possibility that the level of apparent telomere length heterogeneity is artificially elevated due to replication of telomeric DNA during S phase (Wright et al., 1999), we examined the distribution and length of telomeres in interphase nuclei of quiescent (noncycling) cells maintained at high-density confluence as described previously (Nagele et al., 1999). Under these conditions, most cells were densely packed, aligned into parallel arrays and possessed nuclei that were remarkably uniform in shape (Fig. 1A). The extremely flat geometry of these nuclei greatly facilitated visualization and quantitation of fluorescent telomeric subdomains within a very shallow focal depth and, at the same time, minimized the possibility of telomere signal superposition.

Fig. 1B is a representative image showing the distribution of telomeres in quiescent, interphase cells. Telomeres were distributed throughout the flattened nuclei and variations in their signal intensity suggestive of telomere length heterogeneity were evident. There was no apparent correlation between the size and magnitude of the telomere hybridization signal and its distance from the nuclear periphery, indicating that individual differences in telomere signal intensity within nuclei are not caused by local variations in probe access into the interior of the nucleus. To demonstrate the accuracy of the measurement technique, we compared the integrated optical density (IOD) values obtained from telomeres on sister chromosomes at anaphase in cycling populations of IMR90 cells. The rationale for this test is that members of a sister chromatid telomere pair contain the same number of telomeric repeats and, thus, should have identical telomere IOD values when subjected to Q-FISH. We selected cells at mid-anaphase because segregating sister chromosomes could be unambiguously identified. The IOD values of sister chromatid telomeres were found to be highly correlated (Fig. 2) as described previously (Lansdorp et al., 1996; Ziljmans et al., 1997). This observation also indicates that telomere IOD values are directly related to the amount of available telomere

target sequence and that IOD values are accurate representations of relative telomere length, particularly when comparing telomeres in a single cell or in different cells in close proximity that were subjected to the same FISH conditions.

IOD values representing each telomere in a single cell were arranged from lowest to highest, and a curve (=telomere length profile, TLP) was generated for each cell. Representative TLPs for quiescent IMR-90 and IMR-91 cells are shown in Fig. 3A-D, respectively. The overall shape of TLPs was remarkably consistent from cell to cell in a single population and similar in both cell lines. The range of IOD values confirmed the heterogeneity of individual telomere lengths. In most quiescent cells, IOD values across each TLP showed a strong tendency to fall into three distinct ranges or 'steps' (steps 1-3). Surprisingly, mean IOD values for the middle step (step 2) and upper step (step 3) appeared to be an approximate multiple of the mean IOD value for the lowest step (step 1). One possible explanation for this phenomenon is that telomere length in these cells is 'quantally heterogeneous' (i.e. existing only as multiples of a baseline telomere length represented by step 1 values). Another possibility is that IOD values in steps 2 and 3 in each TLP are the result of an extremely close juxtaposition of two or three telomeres, respectively, with each component telomere having an IOD value falling within the range of step 1 and being so closely apposed to its neighboring telomere as to appear as a single, combined telomere signal. This latter possibility is supported by several lines of evidence. First, in all cells examined, there was a clear and consistent relationship between the line slopes for each step, i.e. the slope progressively increased from step 1 to step 3 (Fig. 3A-D). Second, we carried out a number of simulated 'telomere fusions' in which telomeres with IOD values within the range of step 1 were 'fused' randomly to generate simulated IOD values for step 2. Likewise, the simulated step 2 telomere IOD values were again allowed to fuse randomly with another step 1 telomere IOD value to generate a simulated range of IOD values for step 3. Remarkably, the shapes of the resulting simulated TLPs were nearly indistinguishable from those derived from actual telomere measurements (Fig. 3E,F**)**. We also investigated the possibility that some or all of the presumably 'fused' telomeres with higher IOD values are an observational artifact resulting from the visual superposition of spatially separated fluorescent signals along the *Z*-axis (= line of sight). It is noteworthy that the highly flattened geometry of quiescent fibroblast nuclei makes such signal superpositions highly unlikely, and the chance that three telomeres could be so perfectly aligned within the *Z*-axis and visually superimposed within the nucleus is remote. Nevertheless, to eliminate this possibility, digital images of serial optical sections through nuclei of 12 quiescent cells were three-dimensionally reconstructed using Metamorph and examined as stereopairs. Results confirmed that telomeres were distributed throughout the entire volume of the nuclei of quiescent cells (Fig. 4A), as they are in their cycling counterparts (Fig. 4B). In addition, visual superposition of telomere fluorescent signals such as those described above were extremely rare in the highly flattened nuclei and accounted for less than one apparent 'telomere fusion' per cell. Lastly, the step-like TLP for quiescent fibroblasts was independent of the probe used, since parallel Q-FISH analyses carried out on quiescent cells hybridized with digoxigenin-labeled telomere probe (Oncor) and detected with fluorescein isothiocyanate (FITC)-labeled antibodies resulted in similar telomere detection efficiencies and TLPs (data not shown). Collectively, these data suggest that, in quiescent human fibroblasts, a substantial number of telomeres in each cell are in such close proximity that they appear to be fused into doublets or triplets, with the frequency of doublets usually exceeding that of triplets **(**Figs 3A-D, 5). When close telomere juxtapositions (or 'fusions') are factored into counting detectable telomeres per cell, the number comes closer to the expected 92 per normal human diploid cell. However, it should be pointed out that, in most cells, the total number of detectable telomeres was still fewer than 92, an unexplained phenomenon that has been observed repeatedly by others (Hendersen et al., 1996; Lansdorp et al., 1996; Slijepcevic et al., 1997; Sprung et al., 1999b). These variations in the number of detected telomeres were not due to local differences in FISH conditions, since adjacent cells on the same slide also showed these variations. In addition, this discrepancy appears to be independent of the probe used, since parallel FISH analyses carried out on quiescent cells hybridized with a digoxigenin-labeled telomere probe (Oncor, Inc.) and detected with fluorescein isothiocyanate (FITC)-labeled antibodies resulted in similar telomere detection efficiencies (data not shown).

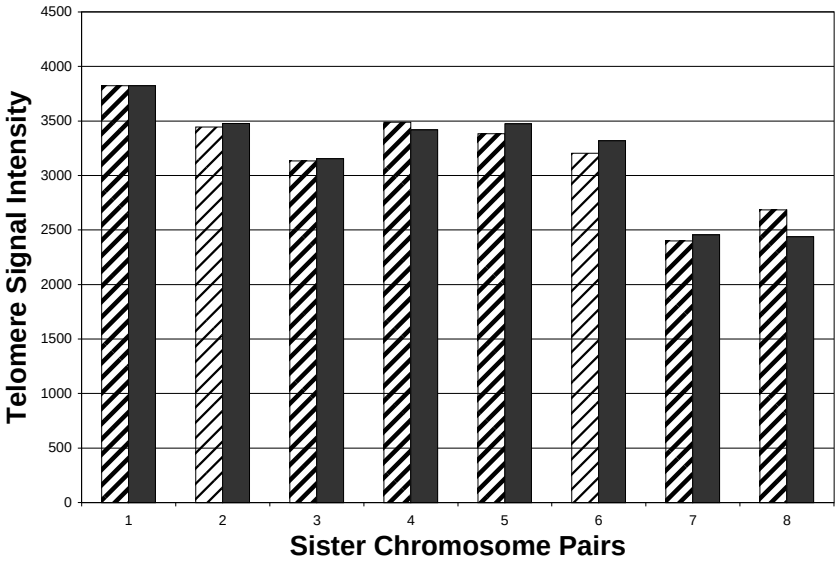

Fig. 2. Comparison of integrated optical density (IOD) values obtained from telomeres on sister chromosomes at anaphase in cycling cell populations showing that IOD values of sister chromatid telomeres are highly correlated. This confirms the accuracy of the Q-FISH measurement technique to determine relative telomere lengths in single cells and shows that IOD values are directly related to the amount of available telomere target sequence.

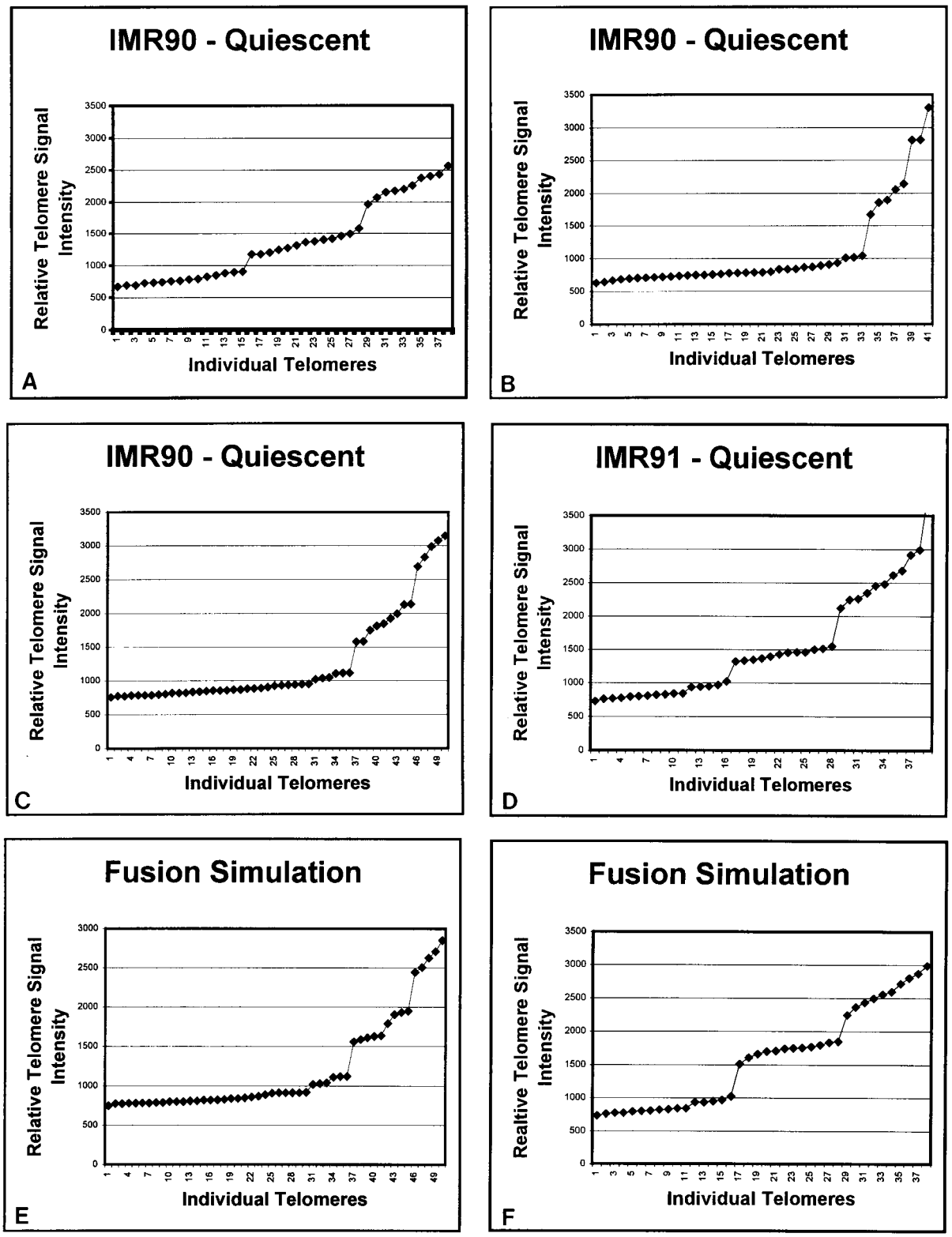

Fig. 3. (A-D) Representative TLPs for single quiescent IMR-90 (A-C) and IMR-91 cells (D). The overall shape of TLPs was remarkably consistent from cell to cell in a single population of quiescent cells and similar in both cell lines. The range of IOD values confirmed the heterogeneity of individual telomere lengths in each cell. IOD values across most TLPs fall into three distinct ranges or 'steps' (steps 1-3), with mean IOD values for the middle step (step 2) and upper step (step 3) being approximate multiples of the mean IOD value for step 1. Line slopes for each step progressively increase from step 1 to step 3. (E-F) Simulated 'telomere fusions' in which telomeres with IOD values within the range of step 1 were 'fused' randomly to generate step 2 IOD values. Simulated step 2 telomere IOD values were also fused randomly with step 1 telomere IOD values to generate step 3 IOD values. Step 1 IOD values from the TLPs shown in C and D were used to generate the simulated TLPs shown in E and F. Resulting simulated TLPs (E,F) were nearly indistinguishable from those derived from actual telomere measurements (C,D).

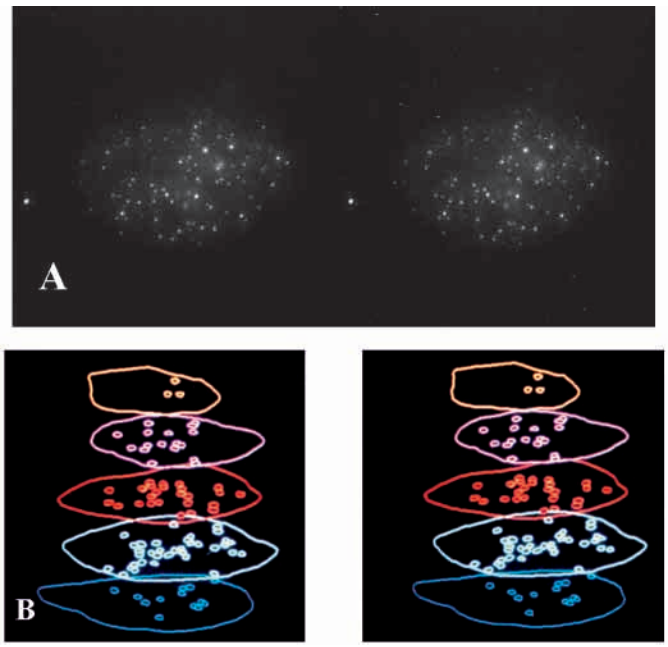

Fig. 4. (A) Stereopair images of a 3D reconstruction of serial optical sections through the nucleus of a representative quiescent human fibroblast, illustrating that telomeres (fluorescent spots) are widely distributed throughout the nucleus. (B) Stereopair images showing the distribution of telomeres within each optical section of a cycling human fibroblast nucleus.

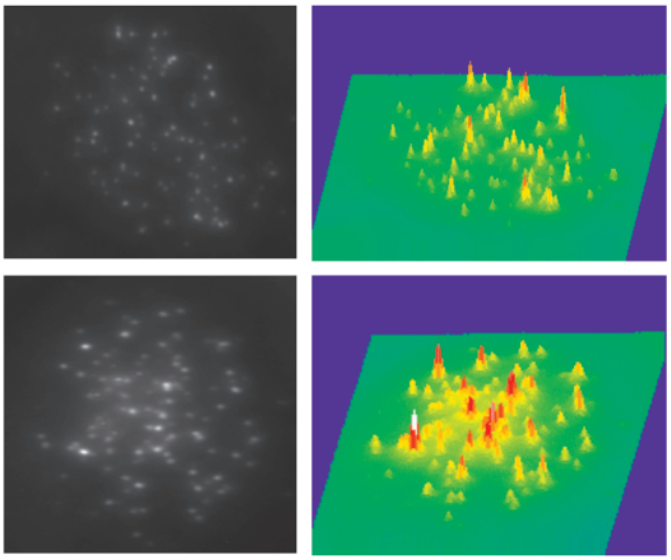

Fig. 5. FISH images (left) and their corresponding fluorescence intensity maps (right) showing the distribution of telomeres and their respective intensities in quiescent human fibroblasts. The height of the peaks in the intensity maps correspond to the signal intensity of individual telomeres, with green, yellow, red and white coloration reflecting a fluorescence intensity roughly corresponding to one, two, three and four telomeres, respectively.

Effect of cell cycle progression on telomere length profiles of individual cells

To determine the effects of variations in cell cycle phase on TLPs, we subcultured quiescent IMR-90 and IMR-91 cells in an effort to remove growth restraints and initiate cycling. Subsequently, we examined the effects of progression through the cell cycle on the TLP using Q-FISH. Since telomeric DNA is replicated throughout S phase (Wright et al., 1999), which occupies roughly 6-8 hours of the 30 hour population doubing time (PDL), the magnitude of IOD values for individual telomeres was expected to vary depending on whether or not telomeric DNA replication had occurred or was in progress at the time of fixation. Our results showed that TLPs are strongly influenced by progression through the cell cycle and often quite variable from cell to cell in a single population. For example, among the asynchronous, cycling cells, 48.4% of interphase nuclei showed TLPs that lacked a step-like pattern (Fig. 6A). It is likely that many of these cells were in S phase at the time of fixation and that some telomere IOD values are increased due to telomeric DNA replication. Nearly 50% (16 out of 31) exhibited a ‘step-like’ TLP comparable to that seen in their quiescent counterparts (Fig. 6B). However, among these, only eight (25.8%) showed the 3-step TLP pattern indicative of telomere juxtaposition or fusion that was predominant among quiescent cells. Another eight cells (25.8%) exhibited TLPs

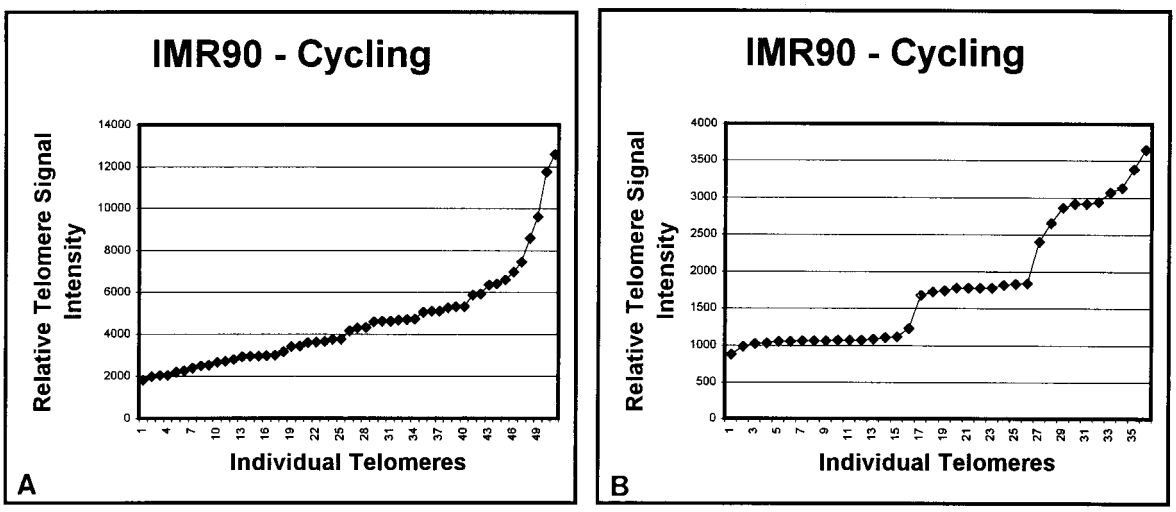

Fig. 6. Representative TLPs of normally cycling IMR90 cells. (A) Roughly half of cycling cells lack a step-like TLP. (B) The remainder exhibit a step-like pattern similar to that seen in quiescent cells.

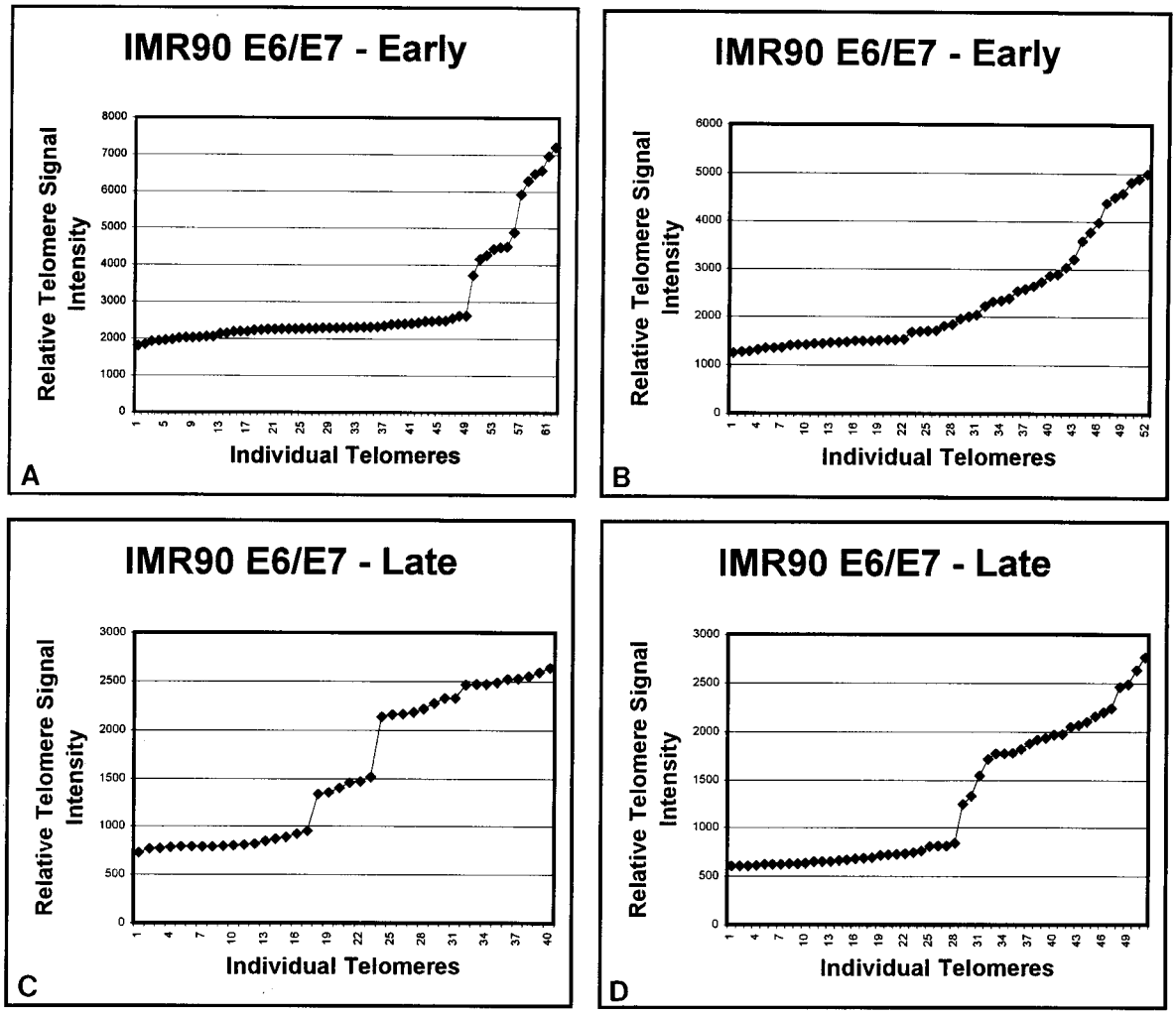

Fig. 7. Effects of telomere shortening on telomere length profiles (TLPs) in early and late passage E6/E7 virus-transformed cells approaching crisis. (A) In early passage cells, a 3-step TLP pattern was found in only 20% of cells. (B) Most early passage cells possessed TLPs showing a more gradual transition of telomere IOD values. (C,D) Late passage cells at or near crisis showed significant telomere shortening, compared to their counterparts at earlier passage, as shown by reduced telomere IOD values. A 3-step TLP pattern (C) comparable to that often seen in quiescent normal cells was found in 5 of the 11 cells that were analyzed, and 2 of 11 cells showed a 2-step TLP pattern (D). Many late-passage cells exhibited morphological features suggesting that they were either cycling slowly or not at all.

with only two distinct steps, suggesting the presence of individual telomeres and telomeres fused into doublets.

Effects of telomere shortening on telomere length profiles in proliferating, virus-transformed cells approaching crisis

Telomeres shorten during replicative aging and following transformation in a variety of human cell types (Wright et al., 1989; Harley et al., 1990; Allsopp et al., 1992; Vaziri et al., 1993; Bodnar et al., 1998). To determine the effects of telomere shortening on TLPs of proliferating, virus-transformed cells approaching crisis, we carried out long-term culturing of telomerase-negative IMR-90 cells that contained the human papilloma virus oncogenes, E6 and E7. These oncogenes have been found to be capable of transforming and immortalizing cells through their interaction with p53 and pRb tumor-suppressor proteins (Munger et al., 1989; Xu, 1996). Cells were subjected to FISH analysis, and we compared the TLPs of interphase, pre-immortal E6/E7 cells at an earlier passage with those at later passage that were driven to crisis. Representative TLPs from cells at early passage are shown in Fig. 7A,B. A discernible 3-step TLP pattern (Fig. 7A) was found only in 20% (2 of 10) of cells, and these cells appeared to be well spread out with morphological features suggesting that they were not cycling. No cells exhibited a 2-step TLP. Other cells possessed TLPs showing a more gradual transition of telomere length IOD values (Fig. 7B). Late passage cells at or near crisis showed significant telomere shortening, as indicated by a reduction in overall telomere signal intensity and IOD values compared to their counterparts at earlier passage. A 3-step TLP pattern comparable to that often seen in quiescent normal cells was found in approximately 45% (5 of 11) of cells at crisis (Fig. 7C), with 18% (2 of 11) of cells showing a 2-step TLP pattern (Fig. 7D). As in these cells at earlier passage, late-passage cells possessed morphological features suggesting that they are either not cycling or are cycling relatively slowly. Surprisingly, despite severe telomere shortening, the slope of the curve representing telomeres IOD

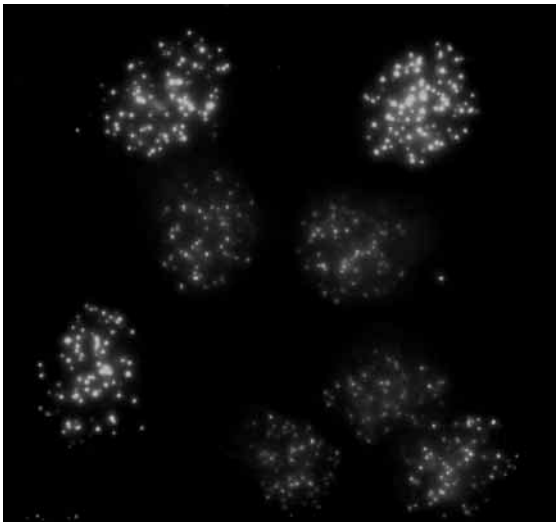

Fig. 8. HeLa S3 cells subjected to FISH with telomere-specific PNA probe showing large variations in telomere signal intensity from cell to cell that may reflect their different proliferative histories or individual variations in the rate of telomere rejuvenation through the activity of telomerase.

values falling into step 1 was comparable to that of their normal, untransformed counterparts. The lack of increased telomere length heterogeneity in step 1 IOD values at this point in the cell's proliferative history strongly suggests that telomere shortening during cell aging and following cell transformation continues to occur progressively and proportionally for most chromosomes. However, in this context, it is noteworthy to add that cultures at or near crisis show extremely long population doubling times as a result of dramatic increase in the rate of cell death.

Effects of telomerase activity on telomere length profiles in immortalized HeLa cells

The 'immortal status' of tumor cells is generally thought to be due, at least in part, to telomere rejuvenation by telomerase. However, it is not yet known whether telomerase activity leads to increased telomere length heterogeneity within individual tumor cells. To address this question and to determine whether telomeric juxtapositions or 'fusions' occur in immortalized cells, we subjected HeLa S3 cells to FISH with telomere-specific PNA probe (Fig. 8**)**. Representative TLPs for HeLa cells are shown in Fig. 9. Only 10% of cells (1 of 10 cells) showed evidence of a step-like TLP pattern comparable to that of normal quiescent IMR-90 and IMR-91 cells (cf. Fig. 3A-D). In the remainder, TLPs revealed considerable telomere length heterogeneity, as shown by the relatively steep slope of the curve (Fig. 9). These results suggest that telomere length maintenance via telomerase activity leads to an increased telomere length heterogeneity in telomerase-positive, immortalized tumor cells. In addition, TLPs of Hela S3 cells revealed that telomere fusions, seen in all of the telomerase-negative, non-immortal cells, are a rare event in immortal cells, despite the increase in chromosome number in these aneuploid cells that might be expected to make such fusion events more likely.

DISCUSSION

Q-FISH allows the generation of telomere length profiles for single cells at interphase

Most of our current knowledge of changes in telomere length associated with replicative aging in normal cells and the activity of telomerase in tumor cells has come from Southern analyses of telomere restriction fragments (TRFs) derived from large populations of cells with different proliferative histories (de Lange et al., 1990; Allshire et al., 1989; Harley et al., 1990), which often results in an exaggeration of telomere length heterogeneity. Thus, Southern analysis provides only an estimate of the average telomere length in the entire cell population (de Lange et al., 1990; Harley et al., 1990; Levy et al., 1992). On the other hand, the Q-FISH method (Lansdorp et al., 1996), which measures the length of individual telomeres and can detect changes in telomere size at the single cell level (Lansdorp et al., 1996; Zijlmans et al., 1997; Poon et al., 1999;

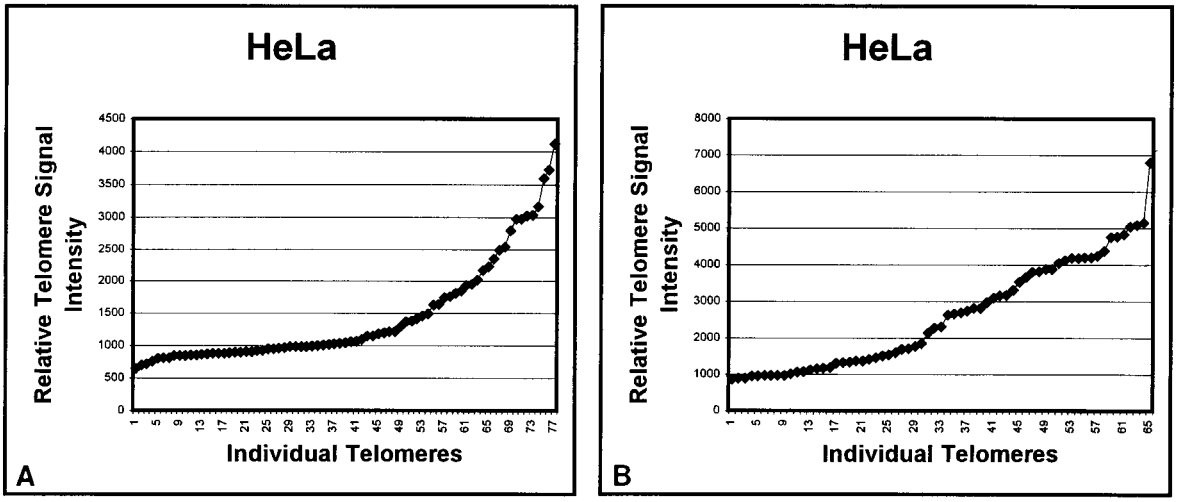

Fig. 9. TLPs in separate immortalized HeLa cells. (A,B) Most TLPs revealed considerable telomere length heterogeneity as shown by the relatively steep slope of the curve and little or no evidence of telomere fusions.

Martens et al., 2000), provides more accurate information about telomere length, telomere dynamics and telomere rejuvenation through the activity of telomerase. To date, most studies using Q-FISH have dealt with analysis of telomere length on isolated chromosomes of metaphase preparations, and few studies have used this or comparable methods to examine telomere length in interphase nuclei (Hendersen et al., 1996). This is not suprising because metaphase preparations offer the following technical advantages: (1) high quality of hybridization without restrictions on access of the probe to the target sequence; (2) the option of assigning a telomere length to an individual, identified chromosome; and (3) avoidance of telomere length variations associated with DNA replication at S phase.

In the present study we used Q-FISH to determine the relative sizes of individual telomeres in cultured human cells under conditions of cell cycling, replicative quiescence, virus-mediated cell transformation and immortalization. We used this data to generate TLPs that display the distribution of relative telomere lengths in a single cell. Individual telomere length values were expressed as relative integrated optical densities (IOD). IOD values were not converted to telomere length expressed in base pairs because telomere standards of known length are not readily incorporated into the cytoplasm of the same cells subjected to telomere length analysis, and hybridization conditions of intranuclear telomeres and extracellular telomere length standards are not considered identical.

Telomere length profiles reveal numerous telomere associations in interphase nuclei of quiescent (noncycling) cells

Henderson et al. (Henderson et al., 1996) examined the length of individual telomeres in intact, interphase nuclei of cultured human cells and demonstrated heterogeneity of telomere length in single cells as well as retention of this heterogeneity during telomere shortening associated with replicative aging. Since telomeres are synthesized throughout S phase in normally cycling cultured cells (Wright et al., 1999), data on telomere length from cells in S phase may be somewhat skewed towards increased telomere length heterogeneity. To circumvent this potential problem, we initially used Q-FISH to examine the distribution and relative length of telomeres in interphase nuclei of quiescent (noncycling) human fibroblasts. These cells were chosen as a model system because they are readily subjected to FISH as intact cells, they are essentially 'locked' in the G_0/G_1 phase of the cell cycle, and they possess a flattened ellipsoidal nucleus of remarkably uniform shape (Nagele et al., 1999). The distribution of telomeres throughout the interphase nuclei of these cells agrees with previous reports of telomere distributions in mammalian cell nuclei (Manuelidis and Borden, 1988; Billia and DeBoni, 1991; Vourc'h et al., 1993), but differs from the telomere distribution seen in many plant cell nuclei, where they often congregate at one pole of the nucleus (Martinez-Perez et al., 1999; Bass et al., 2000; Leitch, 2000). Also, during meiosis in yeast, telomeres form pre-mitotic aggregates, disperse from these aggregates and congregate again to form a 'bouquet arrangement' near the spindle body (Trelles-Sticken et al., 1999), an arrangement that is also seen in mouse spermatocytes (Scherthan et al., 2000). This has led to the suggestion that meiotic telomere clustering may facilitate efficient synaptic pairing of homologues.

Analysis of TLPs for individual quiescent cells confirmed a comparable degree of telomere length heterogeneity among neighboring cells in culture and also revealed a strong tendency for individual telomere IOD values to fall into one of three distinct ranges or 'steps' (steps 1-3) in nearly all cells examined. Surprisingly, mean telomere IOD values for the middle step (step 2) and upper step (step 3) were an approximate multiple of the mean IOD value for the lowest step (step 1), suggesting that the 'quantal' nature of this '3-step' TLP pattern may reflect the fact that the telomeric ends of some chromosomes are fused. To strengthen the possibility that IOD values in steps 2 and 3 represent such telomere 'fusions' or interphase TAs, rather than simply longer telomeres, we were able to reproduce the observed 3-step pattern by simulating random fusions of telomeres with IOD values falling within the range of step 1. The 'quantal' nature of telomere IOD values in steps 2 and 3 and the variable positions of TAs within the nuclear volume argue against observed telomere IOD values being due to local variations in accessibility of the probe. Lastly, examination of stereopair images of 3D reconstructions showed that TAs were not a visual artifact due to the superposition of spatially distinct telomere signals along the line of sight (*Z*-axis). Taken together, these observations have led us to conclude that, in quiescent cells, telomeric ends of chromosomes can be closely juxtaposed during interphase such that fluorescent signals emerging from the point of apparent fusion appear as a single, bright telomere.

Interphase telomere associations are relatively rare in both proliferating virus-transformed cells with shortened telomeres and telomerase-positive, immortalized cells

Telomeres shorten during replicative aging in a wide variety of human cell types (Wright et al., 1989; Harley et al., 1990; Counter et al., 1992; Vaziri et al., 1993; Chiu and Harley, 1997; Bodnar et al., 1998). In the present study, we used successive passages of virus-transformed cells to examine the effects of continued telomere shortening on the number of interphase TAs detected in nuclei. Cell transformation with viral oncogenes results in a bypass of senescence, and these virus-transformed cells eventually succumb to crisis, a period of widespread cellular death due, at least in part, to critical shortening of telomeres (Bodnar et al., 1998; Kiyono et al., 1998). If telomere shortening occurred erratically in these cells during successive rounds of mitosis, the resulting increased level of telomere length heterogeneity would be discernible in single cell TLPs as a change in the slope of the TLP curve. This was, however, not observed when comparing early- and late-passage transformed cells. TLPs revealed that preimmortal E6/E7 transformed cells at or near crisis showed significant, but proportional, telomere shortening, as indicated by a general reduction in telomere signal intensities and corresponding IOD values compared to their counterparts at earlier passage as well as by detection of fewer telomeres per cell. The number of interphase TAs per nucleus and number of nuclei exhibiting TAs in cells at or near crisis increased over that seen in comparable cells at earlier passage. At first glance, this finding agrees with other studies which show that the number of TAs associated with dicentric chromosomes in a variety of mitotic virus-transformed cells, immortalized cells and cells from

patients with ataxia telangiectasia is increased in cells with severely shortened telomeres (Counter et al., 1992; de Lange, 1995; Zakian, 1995; Metcalfe et al., 1996; Ducray et al., 1999; Sprung et al., 1999b). However, since TLPs of quiescent normal diploid cells somewhat resembled those of late-passage E6/E7 virus-transformed cells with severely shortened telomeres, this suggests that the formation of interphase TAs may be independent of telomere length.

The number of interphase telomere associations is correlated with the cell cycling status

Although interphase TAs were most prevalent in nuclei of quiescent (noncycling) normal diploid fibroblasts, and were far less numerous in their rapidly cycling counterparts that possess telomeres of comparable length. This suggests that the formation of interphase TAs is more directly related to the cycling status of the cell than to the specific length of telomeres. Several observations in the present study support this possibility. First, the number of interphase TAs per nucleus did not increase with further telomere shortening in virus-transformed cells near crisis. In fact, as mentioned above, TLPs and the number of interphase TAs in quiescent normal diploid cells and transformed cells near crisis were quite similar, but interphase TAs were relatively rare in transformed cells at earlier passage. It is possible that the increase in the number of interphase TAs seen in late passage virus-transformed cells, rather than their earlier passage counterparts, may be related to the fact that a substantial fraction of the former have ceased proliferating, whereas the latter were still proliferating rapidly. Lastly, interphase TAs were only rarely observed in telomerase-positive, immortalized HeLa cells, which maintain a rather stable telomere length.

It is conceivable that interphase TAs are somehow involved in stabilizing relative chromosome positions within nuclei engaged in a prolonged interphase, and that the relatively short duration of the G_1 phase in rapidly cycling cells may preclude establishment of these TAs. This possibility is supported by our previous study (Nagele et al., 1999) which demonstrated that chromosomes 7, 8, 16, X and Y occupy preferred locations within the nuclei of quiescent diploid and triploid human fibroblasts, but not when these same cells are cycling normally. In agreement with this interpretation, Bridger et al. (Bridger et al., 2000) have demonstrated that the organization of chromosomes in quiescent or senescent mammalian cells is distinctly different from that seen in their proliferating counterparts, suggesting that the spatial organization of the genome changes during transit through the cell cycle. The achievement of stable chromosome positioning within interphase nuclei may also be a common feature of terminally differentiated cell types such as human bronchial epithelial cells (Koss et al., 1998), human leukocytes (Chaudhuri and Reith, 1997) and certain human neurons (Maneulidis, 1984; Manuelidis and Borden, 1988; Martou and De Boni, 2000). The nature of the putative interaction between telomeric ends of associated chromosomes and between TAs and their surrounding nuclear matrix is unknown. Some studies have suggested that components of the nuclear matrix, possibly the nucleoskeleton, anchor chromosomes to preferred intranuclear positions (Mirkovitch et al., 1984; Berezney, 1991; Craig et al., 1997; Nickerson et al., 1997; Pierron and Puvion-Dutilleul, 1999; Weipoltshammer et al., 1999). Telomeres and telomere-specific binding proteins may associate directly with nuclear matrix and participate in anchoring chromosomes to the nuclear envelope and its surrounding nuclear matrix proteins (de Lange, 1992; Luderus et al., 1996; Weipoltshammer et al., 2000). For example, the human telomeric protein TRF2 plays a key role in the protective activity of telomeres (Van Steensel et al., 1998), suggesting that chromosome end fusions and senescence in primary human cells are caused by loss of TRF2 from shortened telomeres. Further work is needed to resolve the potential involvement of telomere-specific binding proteins and nuclear matrix components in the formation and maintenance of interphase TAs. Overall, our results lead us to propose that interphase TAs may play a role in the generation and/or maintenance of nuclear architecture and chromosome positional stability in cells with a prolonged G_1/G_0 phase and perhaps in terminally differentiated cells. Whether or not interphase TAs involve consistent associations among the same chromosomes remains to be determined.

The authors wish to thank Drs Kai-Mon Lee and Kersti Linask for many helpful discussions. Supported by grants to R.N. from the State of New Jersey Commission on Cancer Research and the State of New Jersey Department of Human Services.

REFERENCES

Allshire, R. C., Dempster, M. and Hastie, N. (1989). Human telomeres contain at least three types of G-rich repeat distributed nonrandomly. *Nucl. Acids Res.* **17**, 4611-4627.

Allsopp, R., Vaziri, H., Patterson, C., Goldstein, S., Younglai, E., Futcher, A., Greider, C. and Harley, C. (1992). Telomere length predicts replicative capacity of human fibroblasts. *Proc. Natl. Acad. Sci. USA* **89**, 10114-10118.

Bass, H. W., Riera-Lizarazu, O., Ananiev, E. V., Bordoli, S. J., Rines, H. W., Phillpis, R. L., Sedat, J. W., Agard, D. A. and Cande, W. Z. (2000). Evidence for the coincident initiation of homolog pairing and synapsis during telomere-clustering (bouquet) stage of meiotic prophase. *J. Cell Sci*. **113**,1033-1042.

Bennett, S. and Bennett, M. (1992). Spatial separation of ancestral genomes in the wild grass *Milium montianum* Parl. *Ann. Bot.* **70**, 111-118.

Bereszney, R. (1991). The nuclear matrix: a heuristic model for investigating genomic organization and function in the cell nucleus. *J. Cell. Biochem.* **47**, 109-123.

Billia, F. and deBoni, U. (1991). Localization of centromeric satellite and telomeric DNA sequences in dorsal root ganglion neurons, in vitro. *J. Cell Sci.* **100**, 219-226.

Blackburn, E. (1991). Structure and function of telomeres. *Nature* **350**, 569-573.

Blasco, M. A., Lee, H.-W., Hande, P., Samper, E., Lansdorp, P., DePinho, R. and Greider, C. W. (1997). Telomere shortening and tumor formation by mouse cells lacking telomerase RNA. *Cell* **91**, 25-34.

Bodnar, A. G., Ouellette, M., Frolkis, M., Holt, S. E., Chiu, C.-P., Morin, G. B., Harley, C. B., Shay, J. W., Lichtsteiner, S. and Wright, W. E. (1998). Extension of life-span by introduction of telomerase into normal human cells. *Science* **279**, 349-352.

Bridger, J. M., Boyle, S., Kill, I. R. and Bickmore, W. A. (2000). Re-modeling of nuclear architecture in quiescent and senescent human fibroblasts. *Curr. Biol.* **10**, 149-152.

Callimassia, M. A., Murray, B. G., Hammett, K. R. and Bennett, M. D. (1994). Parental genome separation and asynchronous centromere division in interspecific F1 hybrids in Lathyrus. *Chrom. Res*. **2**, 383-397.

Chaly, N. and Brown, D. (1988). The prometaphase configuration and chromosome order in early mitosis. *J. Cell Sci*. **91**, 325-335.

Chaudhuri, J. P. and Reith, A. (1997). Symmetric chromosomal order in leukocytes indicated by DNA image cytometry and fluorescence in situ hybridization. *Anal. Quant. Cytol. Histol.* **19**, 30-36.

Chiu, C. and Harley, C. (1997). Replicative senescence and cell immortality:

The role of telomeres and telomerase. *Proc. Soc. Exp. Biol. Med.* **214**, 99-105.

Comings, D. E. (1968). The rationale for an ordered arrangement of chromatin in the interphase nucleus. *Am. J. Hum. Genet.* **20**, 440-460.

Comings, D. E. (1980). Arrangement of chromatin in the nucleus. *Hum. Genet.* **53**, 131-143.

Costello, D. (1970). Identical linear order of chromosomes in both gametes of the Acoel *Turbellarian polychoerus carmelensis*: a preliminary note. *Proc. Natl. Acad. Sci. USA* **67**, 1951-1958.

Counter, C. M., Avilion, A. A., LeFeuvre, C. E., Stewart, N. G., Greider, C. W., Harley, C. B. and Bacchetti, S. (1992). Telomere shortening associated with chromosome instability is arrested in immortal cells which express telomerase activity. *EMBO J.* **11**, 1921-1929.

Craig, J. M., Boyle, S., Perry, P. and Bickmore, W. A. (1997). Scaffold attachments within the human genome. *J. Cell Sci*. **110**, 2673-2682.

Croft, J. A., Bridger, J. M., Boyle, S., Teague, P. and Bickmore, W. A. (1999). Differences in the localization and morphology of chromosomes in the human nucleus. *J. Cell Biol*. **145**, 1119-1131.

De Lange, T. (1992). Human telomeres are attached to the nuclear matrix. *EMBO J.* **11**, 717-724.

De Lange, T., Shiue L., Myers R. M., Cox D. R., Naylor S. L., Killery A. M. and Varmus H. E. (1990). Structure and variability of human chromosome ends. *Mol. Cell. Biol*. **10**, 518-527.

De Lange, T. (1995). Telomere dynamics and genome instability in human cancer. In *Telomeres*, pp. 265-293. Cold Spring Harbor, NY: Cold Spring Harbor Press.

Ducray, C., Pommier, J. P., Martins, L., Boussin, F. D. and Sabatier, L. (1999). Telomere dynamics, end-to-end fusions and telomerase activation during the human fibroblast immortalization process. *Oncogene* **18**, 4211-4223.

DuPraw, E. (1970). *DNA and Chromosomes*. New York: Holt, Rinehart and Winston.

Egholm, M., Buchardt, O., Christensen, L., Behrens, C., Freier, S. M., Driver, D. A., Berg, R. H., Kim, S. K., Norden, B., Nielsen, P. E. (1993). PNA hybridizes to complementary oligonucleotides obeying the Watson-Crick hydrogen-bonding rules. *Nature* **365**, 566-568.

Haaf, T. and Schmid, M. (1991). Chromosome topology in mammalian interphase nuclei. *Exp. Cell Res.* **192**, 325-332.

Hande, M. P., Samper, E., Lansdorp, P. and Blasco, M. A. (1999). Telomere length dynamics and chromosomal instability in cells derived from telomerase null mice. *J. Cell Biol.* **144**, 589-601.

Harley, C. B., Futcher, A. B. and Greider, C. W. (1990). Telomeres shorten during aging of human fibroblasts. *Nature* **345**, 458-460.

Hastie, N. and Allshire, R. (1989). Human telomeres: fusion and interstitial sites. *Trends Genet.* **5**, 326-331.

Henderson, S., Allsopp, R., Spector, D., Wang, S. and Harley, C. (1996). In situ analysis of changes in telomere size during replicative aging and cell transformation. *J. Cell Biol*. **134**, 1-12.

Heslop-Harrison, J. S. and Bennett, M. D. (1984). Chromosome order – possible implications for development. *J. Embryol. Exp. Morphol.* **83**, 51-73.

Kiyono, T., Foster, S. A., Koop, J. I., McDougall, J. K., Galloway, D. A. and Klingelhutz, A. J. (1998). Both Rb/p16INK4a inactivation and telomerase activity are required to immortalize human epithelial cells. *Nature* **396**, 84-88.

Klein, C., Cheutin, T., O'Donohue, M., Rothblum, L., Kaplan, H., Beorchia, A., Lucas, L, Heliot, L and Ploton, D. (1998). The three-dimensional study of chromosomes and upstream binding factor-immunolabeled nucleolar organizer regions demonstrates their nonrandom spatial arrangement during mitosis. *Mol. Biol. Cell* **9**, 3147-3159.

Koss, L. G. (1998). Characteristics of chromosomes in polarized normal human bronchial cells provide a blueprint for nuclear organization. *Cytogenet. Cell Genet.* **82**, 230-237.

Lansdorp, P. M., Verwoerd, N. P., van de Rijke, F. M., Dragowska, V., Little, M. T., Dirks, R. W., Raap, A. K. and Tanke, H. J. (1996). Heterogeneity in telomere length of human chromosomes. *Hum. Mol. Genet.* **5**, 685-691.

Leitch, A., Brown, J., Mosgoller, W., Schwarzacher, T. and Heslop-Harrison, J. (1994). The spatial localization of homologous chromosomes in human fibroblasts at mitosis. *Hum. Genet*. **93**, 275-280.

Leitch, A., Schwarzacher, T., Mosgoller, W., Bennett, M. and Heslop-Harrison, J. (1991). Parental genomes are separated throughout the cell cycle in a plant hybrid. *Chromosoma* **101**, 206-213.

Leitch, A. R. (2000). Higher levels of organization in the interphase nucleus of cycling and differentiated cells. *Micro. Molec. Biol. Rev.* **64**, 138-152.

Levy, M., Allsopp, R., Futcher, A., Greider, C. and Harley, C. (1992). Telomere end-replication problem and cell aging. *J. Mol. Biol.* **225**, 951-960.

Luderus, M. E., van Steensel, B., Chong, L., Sibon, O. C., Cremers, F. F. and de Lange, T. (1996). Structure, subnuclear distribution, and nuclear matrix association of the mammalian telomeric complex. *J. Cell Biol*. **135**, 867-881.

Manuelidis, L. (1984). Different central nervous system cell types display distinct and nonrandom arrangements of satellite DNA sequences. *Proc. Natl. Acad. Sci. USA* **81**, 3123-3127.

Manuelidis, L. (1990). A view of interphase chromosomes. *Science* **250**, 1533-1540.

Manuelidis, L. and Borden, J. (1988). Reproducible compartmentalization of individual chromosome domains in human CNS cells revealed by in situ hybridization and three-dimensional reconstruction. *Chromosoma* **96**, 397-410.

Martens, U. M., Chavez, E. A., Poon, S. S., Schmoor, C. and Lansdorp, P. M. (2000). Accumulation of short telomeres in human fibroblasts prior to replicative senescence. *Exp. Cell Res.* **256**, 291-299.

Martinez-Perez, E., Shaw, P., Reader, S., Aragon-Alcaide, L., Miller, T. and Moore, T. (1999). Homologous chromosome pairing in wheat. *J. Cell Sci*. **112**,1761-1769.

Martou, G. and De Boni, U. (2000). Nuclear topology of murine, cerebellar Purkinje neurons: changes as a function of development. *Exp. Cell Res.* **256**, 131-139.

Mayer, W., Smith, A., Fundele, R. and Haaf, T. (2000). Spatial separation of parental genomes in preimplantation mouse embryos. *J. Cell Biol.* **148**, 629-634.

McClintock, B. (1941). The stability of broken ends of chromosomes in *Zea mays*. *Genetics* **26**, 234-282.

Meyne, J., Ratliff, R. and Moyzis, R. (1989). Conservation of the human telomere sequence (TTAGGG)n among vertebrates. *Proc. Natl. Acad. Sci. USA* **86**, 7049-7053.

Metcalfe, J. A., Parkhill, J., Campbell, Y., Stacey, M., Biggs, P., Byrd, P. J. and Taylor, A. M. (1996). Accelerated telomere shortening in Ataxia Telangiectasia. *Nat. Genet.* **13**, 350-353.

Mirkovitch, J., Mirault, M. E. and Laemmli, U. K. (1984). Organization of the higher order chromatin loop: specific DNA attachment sites on nuclear scaffold. *Cell* **39**, 223-232.

Mosgoller, W., Leitch, A., Brown, J. and Heslop-Harrison, J. (1991). Chromosome arrangements in human fibroblasts at mitosis. *Hum. Genet*. **88**, 27-33.

Munger K., Phelps, W. C., Bubb, V., Howley, P. M. and Schlegel, R. (1989). The E6 and E7 genes of the human papilloma virus type 16 together are necessary and sufficient for transformation of primary human keratinocytes. *J. Virol.* **63**, 4417-4421.

Nagele, R. G., Bush, K., Huff, D. and Lee, H. (1992). Computer-assisted three-dimensional reconstruction and dissection. *Meth. Neurosci.* **10**, 492-502.

Nagele, R., Freeman, T., McMorrow, L. and Lee, H. (1995). Precise spatial positioning of chromosomes during prometaphase: evidence for chromosome order in human cells. *Science* **270**, 1831-1835.

Nagele, R., Freeman, T., Fazekas, J., Tejera, Z. and Lee, H. (1998). Chromosome spatial order in human cells: evidence for early origin and faithful propagation. *Chromosoma* **107**, 330-338.

Nagele, R. G., Freeman, T., McMorrow, L., Thomson, Z., Kitson-Wind, K. and Lee, H. (1999). Chromosomes exhibit preferential positioning in nuclei of quiescent human cells. *J. Cell Sci.* **112**, 525-535.

Nickerson, J. A., Krochmalnic, G., Wan, K. M. and Penman, S. (1977). The nuclear matrix revealed by eluting chromatin from a crosslinked nucleus. *Proc. Natl. Acad. Sci. USA* **94**, 4446-4450.

Pierron, G. and Puvion-Dutilleul, F. (1999). An anchorage nuclear structure for telomeric DNA repeats in HeLa cells. *Chromosome Res.* **7**, 581-592.

Poon, S. S., Martens, U. M., Ward, R. K. and Lansdorp, P. M. (1999). Telomere length measurements using digital fluorescence microscopy. *Cytometry* **36**, 267-278.

Sandell, L. L. and Zakian, V. A. (1993). Loss of a yeast telomere: arrest, recovery and chromosome loss. *Cell* **75**, 729-739.

Schwarzacher, T., Heslop-Harrison, J., Anamthawat-Jonsson, K., Finch, R. and Bennett, M. (1992). Parental genome separation in reconstructions of somatic and premeiotic metaphases of *Hordeum vulgare* × *H. bulbosum*. *J. Cell Sci.* **101**, 13-24.

Scherthan, H., Jerratsch, M., Dhar, S., Wang, Y. A., Goff, S. P. and

Pandita, T. K. (2000). Meiotic telomere distribution and sertoli cell nuclear architecture are altered in atm- and atm-p53-deficient mice. *Mol. Cell Biol*. **20**,7773-7783.

Slijepcevic, P., Hande, M. P., Bouffler, S. D., Lansdorp, P. and Bryant, P. E. (1997). Telomere length, chromatin structure, and chromosome fusigenic potential. *Chromosoma* **106**, 413-421.

Spector, D. (1993). Macromolecular domains within the cell nucleus. *Annu. Rev. Cell Biol.* **9**, 265-315.

Sprung, C. N., Sabatier, L. and Murnane, J. P. (1999a). Telomere dynamics in a human cancer cell line. *Exp. Cell Res.* **247**, 29-37.

Sprung, C. N., Afshar, G., Chavez, E. A., Lansdorp, P., Sabatier, L. and Murnane, J. P. (1999b). Telomere instability in a human cancer cell line. *Mutat. Res.* **429**, 209-223.

Sun, H. B. and Yokota, H. (1999). Correlated positioning of homologous chromosomes in daughter fibroblast cells. *Chromosome Res.* **7**, 603-610.

Trelles-Sticken, E., Loidl, J. and Scherthan, H. (1999). Bouquet formation in budding yeast; initiation of recombination is not required for meiotic telomere clustering. *J. Cell Sci*. **112**,651-658.

Van Steensel, B., Smogorzewska, A. and de Lange, T. (1998). TRF2 protects human telomeres from end-to-end fusions. *Cell* **92**, 401-413.

Vaziri, H., Dragowska, W., Allsopp, R., Thomas, T., Harley, C. and Lansdorp, P. (1994). Evidence for a mitotic clock in human hemopoietic stem cells: loss of telomeric DNA with age. *Proc. Natl. Acad. Sci. USA* **91**, 9857-9860.

Vourc'h, C., Taruscio, D., Boyle, A. and Ward, D. (1993). Cell cycle-dependent distribution of telomeres, centromeres and chromsomoe-specific subsatellite domains in the interphase nucleus of mouse lymphocytes. *Exp. Cell Res.* **205**, 142-151.

Wan, T. S. K., Martens, U. M., Poon, S. S. S., Tsao, S.-W., Chan, L. C. and Lansdorp, P. M. (1999). Absence or low number of telomere repeats at junctions of dicentric chromosomes. *Genes Chromosomes Cancer* **24**, 83-86.

Weipoltshammer, K., Schofer, C., Almeder, M., Philimonenko, V. V., Frei, K., Wachtler, F. and Hozak, P. (1999). Intranuclear anchoring of repetitive DNA sequences: centromeres, telomeres and ribosomal DNA. *J. Cell Biol.* **147**, 1409-1418.

Wright, W., Pereira-Smith, O. and Shay, J. (1989). Reversible cellular senescence: implications of normal human diploid fibroblasts. *Mol. Cell Biol.* **9**, 3088-3092.

Wright, W. E., Tesmer, V. M., Liao, M. L. and Shay, J. W. (1999). Normal human telomeres are not late replicating. *Exp. Cell Res.* **251**, 492-499.

Xu, F. P. (1996). The human papillomavirus E6/E7 genes induce discordant changes in the expression of cell growth regulatory proteins. *Carcinogenesis* **17**, 1395-1401.

Zakian, V. (1989). Structure and function of telomeres. *Annu. Rev. Genet.* **23**, 579-560.

Zakian, V. A. (1995). Telomeres: Beginning to understand the end. *Science* **270**, 1601-1607.

Zijlmans, J. M., Martens, U. M., Poon, S., Raap, A. K., Tanke, H. J., Ward, R. K. and Lansdorp, P. M. (1997). Telomeres in the mouse have large inter-chromosomal variations in the number of T2AG3 repeats. *Proc. Natl. Acad. Sci. USA* **94**, 7423-7428.